NEAR-FAULT PULSE IDENTIFICATION IN KUMAMOTO EARTHQUAKE RECORDS

Shubham TRIVEDI[1)] and Hitoshi SHIOHARA[2)]

1) Ph.D. Student, Department of Architecture,
The University of Tokyo, Tokyo, Japan, shubham@rcs.arch.t.u-tokyo.ac.jp
2) JAEE member, Professor, Department of Architecture,
The University of Tokyo, Tokyo, Japan, shiohara@arch.t.u-tokyo.ac.jp

ABSTRACT: A response-spectrum based pulse identification scheme is used to analyze ground motions recorded in 2016, April 16 Kumamoto Earthquake main-shock for the presence of characteristic pulse-like features often observed in near-fault zones of large earthquakes. Pulse-identification is carried out in multiple orientations covering the full 360° compass. Records observed from along the propagating fault are found to contain significant pulse-like component, especially in of the orientations.

Key Words: Near-Fault Earthquakes, Pulse Identification, 2016 Kumamoto Earthquake

1 INTRODUCTION

Ground motions recorded close to the earthquake source have been observed in the past[1)] to have a significant pulse-like component. Identification of such peculiar characteristics of earthquake ground motions may allow for better understanding of seismic demands in zones of high vulnerabilities.

A number of ground motions recorded in the near-fault zone during the 2016, April 16 Kumamoto earthquake are analyzed in this study for identification of pulse-like characteristics. A response spectrum based pulse identification scheme[2)] utilized in this study is briefly explained. Selection criteria of the available ground motions is detailed and the pulse characteristics obtained from analysis are presented.

1.1 Pulse-Indentification Scheme

In this scheme, the dominant pulse-like component of ground motion is represented by a simple single-cycle sinusoidal pulse as expressed by equation (1), where $\dot{u}_P$ is the velocity time-history, V_P is the peak velocity, T_P is the period, and t_s is the starting position of the representative pulse, and t_f is the total length of the ground motion record. Pulse defining parameters (T_P, V_P and t_s) are selected such that the identified simple pulse is sufficiently representative of the ground motion time-history and the response spectrum simultaneously.

$$\dot{u}_P(t) = \begin{cases} V_P \sin\left(\frac{2\pi}{T_P}(t - t_s)\right) & t \in [t_s, t_s + T_P] \\ 0 & t \in [0, t_s) \cup (t_s + T_P, t_f] \end{cases} \tag{1}$$

Compatibility of the response spectrum of ground motion with that of representative pulse is ensured by choosing the V_P for a given T_P such that the peak of representative pulse velocity response spectrum coincides with the velocity response spectrum coordinate of the ground motion at the selected frequency.

For each given T_P (and corresponding V_P,) t_s is determined by optimizing the fit of the pulse waveform to the ground motion waveform as expressed in equation (2) where $\dot{u}_R$ is the residual ground motion obtained by deducting the pulse motion ($\dot{u}_P$) from the given ground motion time-history.

$$\alpha(t_s, T_P) = \int_0^{t_f} \dot{u}_R^2(t)\,\mathrm{d}t \tag{2}$$

Finally, T_P is selected as the time period for which the representative pulse corresponds with the greatest portion of ground motion energy. This is accomplished by choosing the T_P which results in the lowest residual energy ratio (E_R) as expressed by equation (3).

$$E_R(T_P) = \frac{\int_0^{t_f} \dot{u}_R^2(t)\,\mathrm{d}t}{\int_0^{t_f} \dot{u}_P^2(t)\,\mathrm{d}t} \tag{3}$$

2 GROUND MOTION RECORDS

Strong-motion data was recorded at a number of stations in the Kumamoto earthquake of 16 April, 2016 including multiple locations in close proximity to the earthquake epicenter. Selected motion histories recorded within about 15 km of the earthquake epicenter are analyzed in this study for the identification of a coherent pulse-like component. Unprocessed ground motion records have been obtained from the instruments installed by National Research Institute for Earth Science and Disaster Resilience [3)], Japan Meteorological Agency [4)], and Kumamoto Prefecture Local Government [5)]. Geographic locations of the recording stations as described in the respective data sources are expressed on local in figure 1. Also shown on the map are the active fault lines in the region (Futagawa and Hinagu faults) as identified by National Institute of Advanced Industrial Science and Technology [6)] and the epicenters of aftershocks observed after the earthquake. Distances of recoding stations from the epicenter (D_e) and the Station IDs of respective recording stations are listed in table 1. It must be noted that a number of records are available from very close to the epicenter and from either sides of the epicenter along the fault.

Seq. No.	Record Provider	Station ID	Station Name	D_e(km)
1	JMA	EEB	Kasuga, Nishi-ku, Kumamoto-shi	7.5
2	JMA	9CF	Matsubase, Matsubase-machi, Uki-shi	14.2
3	JMA	93048	Komori, Nishihara-mura, Aso-shi	15.8
4	JMA	93051	Miyazono, Mashiki-machi, Kamimashiki-gun	6.4
5	K-NET	KMM006	Kumamoto	5.0
6	K-NET	KMM008	Uto	12.0
7	KiK-net	KMMH14	Toyono	13.0
8	KiK-net	KMMH16	Mashiki	7.0

Table 1: Ground motion records utilized for pulse-identification in present study

Unprocessed acceleration records obtained from the aforementioned sources have been processed by applying a low pass filter with cut-off at 6 s and roll-off at 10 s. Thus filtered acceleration records are used for calculating velocity and displacement time histories required for pulse-identification.

3 ANALYSIS AND DISCUSSION

Pulse-identification scheme described in section 1.1 is utlilized to analyze the ground motion records listed in section 2. This section details the analysis being carried out in multiple ground motion ori-

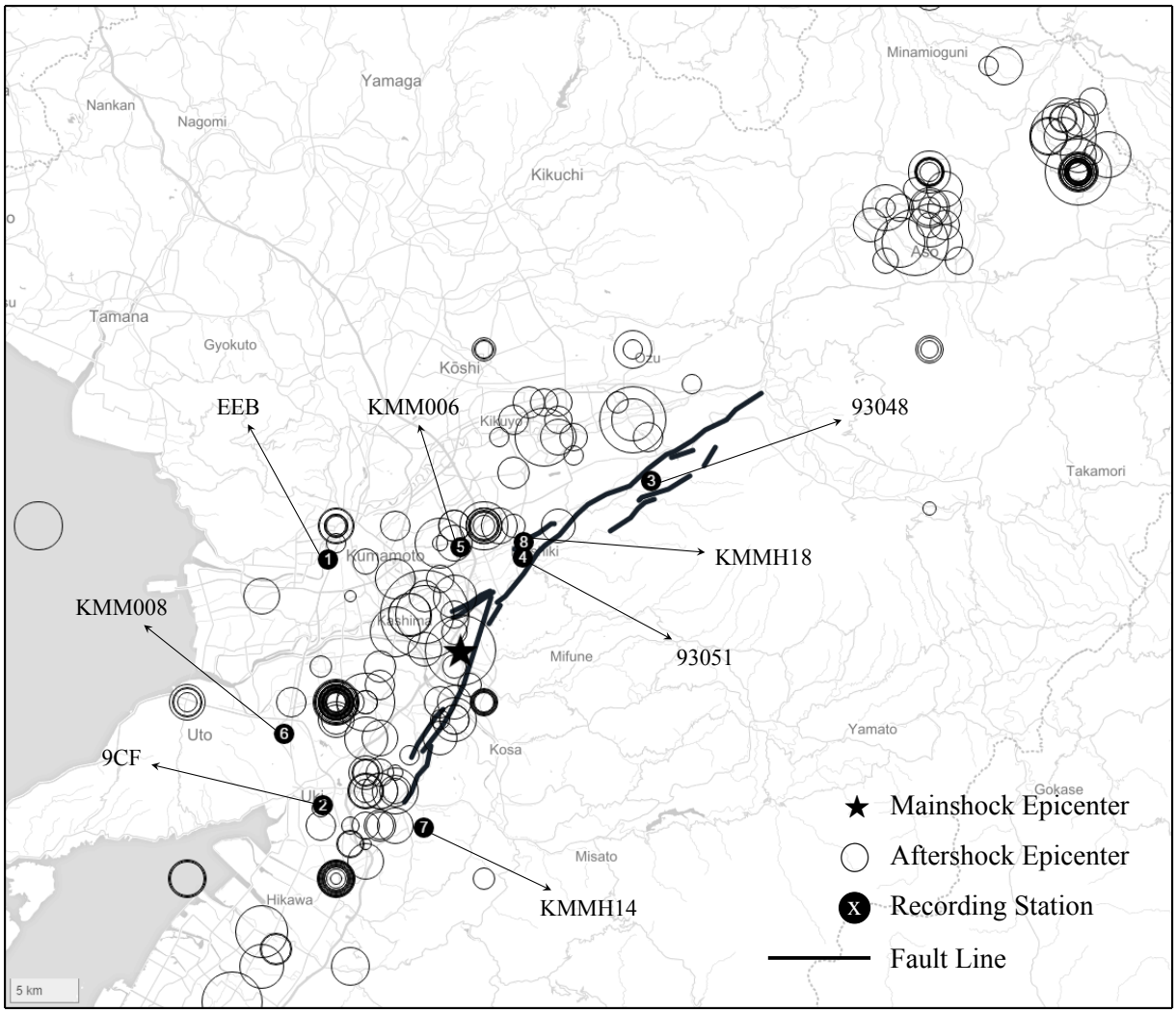

Figure 1: Geographic location of the recording stations and earthquake epicenter

entations and discusses the results in context of the fault direction. Identified pulses in the appropriate direction at each recording station are then expressed.

3.1 Pulse-identification in multiple orientations

Near-fault pulses have been identified in the past researches to be a directional phenomenon[7]. Pulse like features are often observed only in the fault-normal direction while the fault-parallel direction is found to contain no identifiable pulse component. In order to evaluate directivity in the Kumamoto earthquake, pulse identification is carried out in multiple orientations derived from the recorded north-south and east-west components. Ground motion in any required orientation may be expressed as:

$$\ddot{X}_{g_\theta} = \ddot{X}_{g_{EW}} \cos\theta + \ddot{X}_{g_{NS}} \sin\theta \tag{4}$$

where $\ddot{X}_{g_{EW}}$ and $\ddot{X}_{g_{NS}}$ are the east-west and north-south components respectively of the recorded ground acceleration, while $\ddot{X}_{g_\theta}$ is the ground acceleration component at an orientation θ degrees from the east-west direction.

Pulse identification is performed for each ground motion at every 5° orientation over the entire 360° compass. Residual energy ratio (E_R, see section 1.1) thus calculated is expressed in figure 2. It may be

noted that a lower E_R value indicates greater dominance of pulse in the given ground motion. Dotted diameter on the figure highlights the orientation with lowest E_R for each record. Pulse period (T_P) for each ground motion is defined as the T_P corresponding to the orientation with lowest E_R. T_P thus determined along with the corresponding orientations (θ) and E_R values for each ground motion are expressed in table 2. As seen from figure 2, some records (#3, #4, #5, and #8) exhibit significant directivity i.e., E_R value in one of the directions is observed to be significantly more than other directions. Maximum and minimum values of E_R are observed for these records at approximately perpendicular orientations. The orientation with lowest E_R for these records can be generally identified as the NW-SE direction. Referring back to the fault lines and aftershock epicenters in figure 1, this orientation can be identified to be nearly perpendicular to the NE-SW direction of the propagating fault. This observation thus confirms with previous findings that pulse-like features are observed in the fault-normal direction only[7].

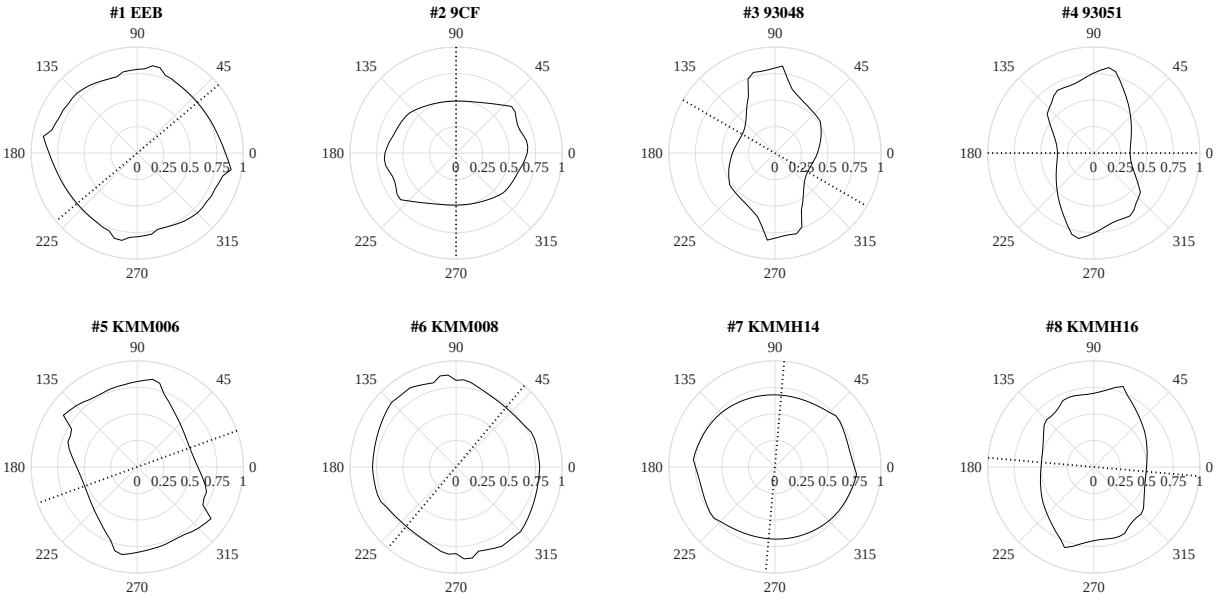

Figure 2: Minimum E_R values obtained through pulse-identification scheme at each orientation (θ)

			Minimum		Maximum		Difference
Seq. No.	Station ID	T_P(s)	$E_{R_{mn}}$	θ_{mn}	$E_{R_{mx}}$	θ_{mn}	$(E_{R_{mx}} - E_{R_{mn}})$
1	EEB	2.02	0.74	40°	0.89	170°	0.15
2	9CF	1.15	0.49	90°	0.68	40°	0.19
3	93048	2.85	0.35	150°	0.82	85°	0.46
4	93051	1.44	0.34	180°	0.81	80°	0.47
5	KMM006	1.75	0.52	20°	0.85	145°	0.32
6	KMM008	0.97	0.73	50°	0.86	100°	0.13
7	KMMH14	1.29	0.67	85°	0.77	175°	0.09
8	KMMH16	1.21	0.49	175°	0.81	70°	0.31

Table 2: Results of pulse-identification over multiple orientations

Further, the minimum E_R value observed for these records is also much lower when compared to other records with no directivity, implying greater pulse-like nature of these records. Referring to the geographic locations where these motions were recorded (figure 1,) it may be noted that all these records are observed on the same side of the earthquake along the propagating fault. Other stations where no

directivity was observed are situated on the opposite end. This observation confirms with previous studies[8] which found pulse-like features in the direction of propagating fault only. Comparing stations #1 and #3, pulse-like strongly observed at station #3 even though it is located at a farther distance from the epicenter but along the fault propagation direction while station #1 exhibits much lower pulse-like nature even though it is located at a much closer distance to the epicenter but opposite the fault propagation direction.

3.2 Identified pulse at the selected orientation

For the orientation identified with minimum value of E_R for each record, detailed pulse-calculations are carried and the resulting pulses and response spectrums are expressed in figures 3 to 10. All figures show the acceleration, velocity, and displacement time-history of the original motion superimposed by the identified pulse in the first column. A zoomed-in view of the respective time-histories is also shown for better reference in the second column. Finally, the third column shows acceleration, velocity, and displacement response spectrums for the ground motions and the identified simple pulse. Identified pulses for records #3, #4, #5, and #8 are particularly observed to be representative to their respective ground motion time histories.

4 CONCLUSIONS

In this study, a number of ground motions recorded during the 2016 Kumamoto Earthquake are analyzed for the presence of characteristic near-fault pulses using a response-spectrum based pulse identification scheme. Results of this analysis may be summarized as follows:

1. Pulse-like features are strongly observed for the records located along the direction of fault propagation as compared to the records obtained in other directions.
2. Generally, pulse-like features are more significantly observed in the fault-normal direction for these records.
3. Records from along the propagating fault are observed to be more pulse-like than the records from a closer distance but opposite the side of earthquake epicenter.
4. Pulse period (T_P) for the analyzed records is generally in the range of 1.2 to 2.8 seconds.
5. Pulses identified with the response-spectrum pulse identification scheme are found to offer a good representation to both, the ground motion time-history and the response spectrum.

REFERENCES

1) Paul G. Somerville, Nancy F. Smith, Robert W. Graves, and Norman A. Abrahamson. Modification of Empirical Strong Ground Motion Attenuation Relations to Include the Amplitude and Duration Effects of Rupture Directivity. *Seismological Research Letters*, 68(1):199–222, January 1997. ISSN 0895-0695, 1938-2057. doi: 10.1785/gssrl.68.1.199. URL http://srl.geoscienceworld.org/content/68/1/199.

2) Shubham Trivedi and Hitoshi Shiohara. Response-spectrum based pulse identification for near-fault earthquake ground motions. In *Proceedings of the AIJ Annual Convention 2016*, in press.

3) National Research Institute for Earth Science and Disaster Resilience (NIED). Strong-motion seismograph networks (K-NET, KiK-net). URL http://www.kyoshin.bosai.go.jp/. Accessed: 2016-06-17.

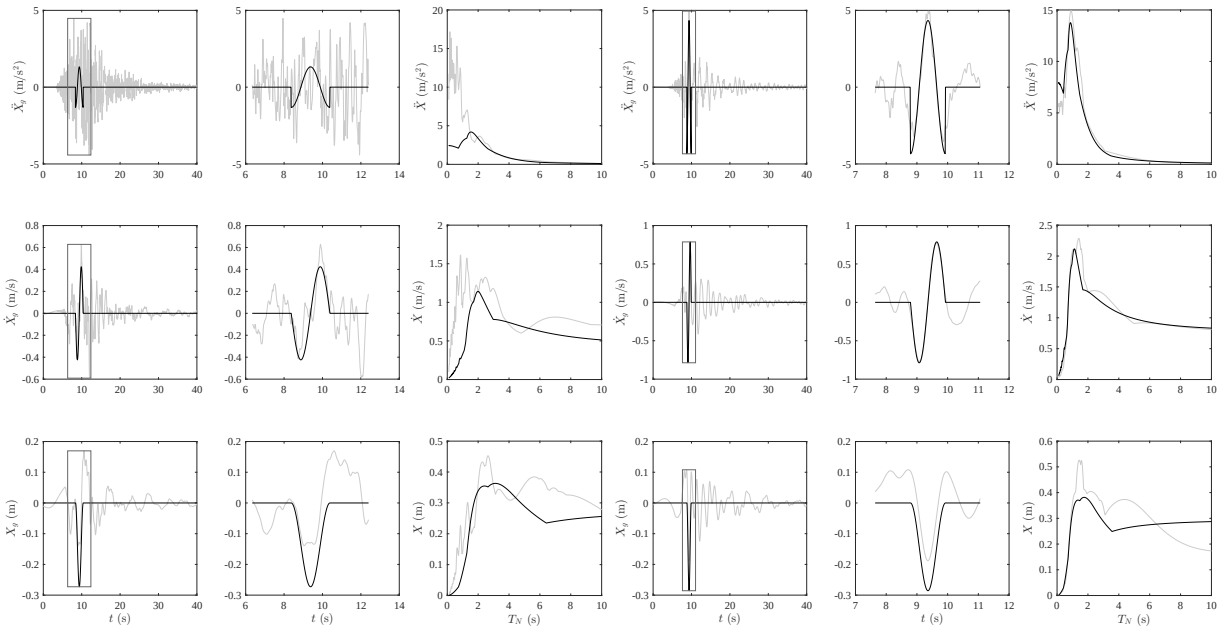

Figure 3: Identified pulse for the EEB record

Figure 4: Identified pulse for the 9CF record

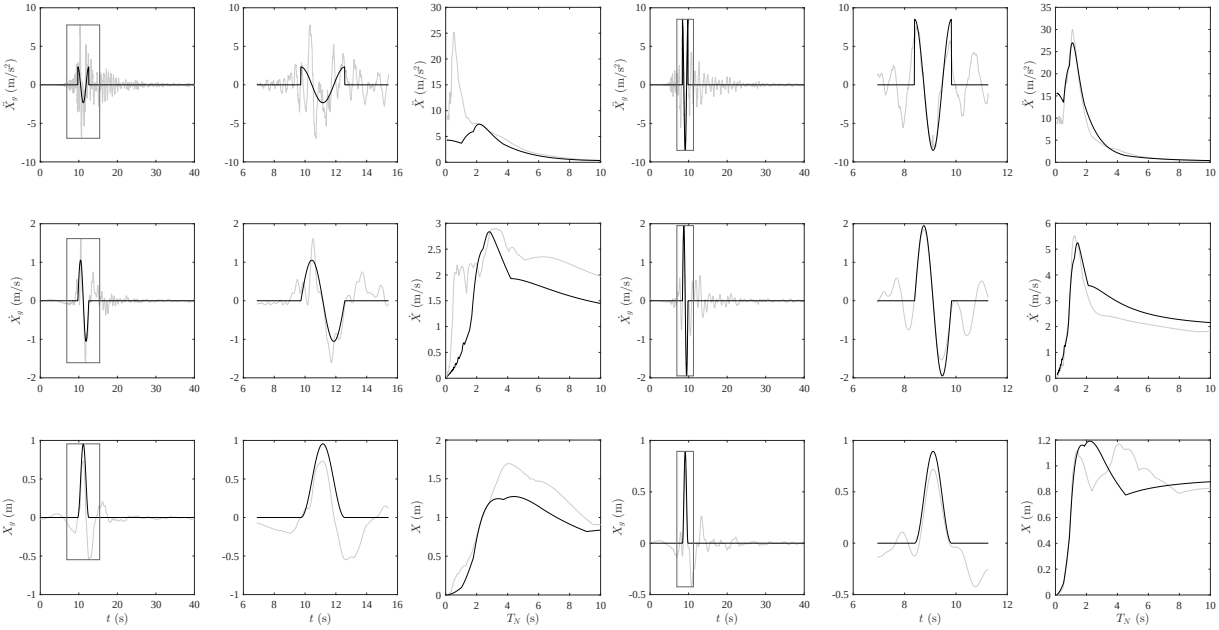

Figure 5: Identified pulse for the 93048 record

Figure 6: Identified pulse for the 93051 record

4) Japan Meteorological Agency (JMA). Strong ground motion data for Kumamoto earthquake. URL http://www.data.jma.go.jp/svd/eqev/data/kyoshin/jishin/160416_kumamoto/index.html. Accessed: 2016-06-17.

5) Kumamoto Prefecture Local Government. Local government ground motion data. URL http://www.data.jma.go.jp/svd/eqev/data/kyoshin/jishin/160416_kumamoto/index2.html. Accessed: 2016-06-17.

6) National Institute of Advanced Industrial Science and Technology (AIST). Active Fault Database of Japan [Research Information Database DB095], 2012. URL https://gbank.gsj.jp/activefault/index_e_gmap.html. Accessed: 2016-06-17.

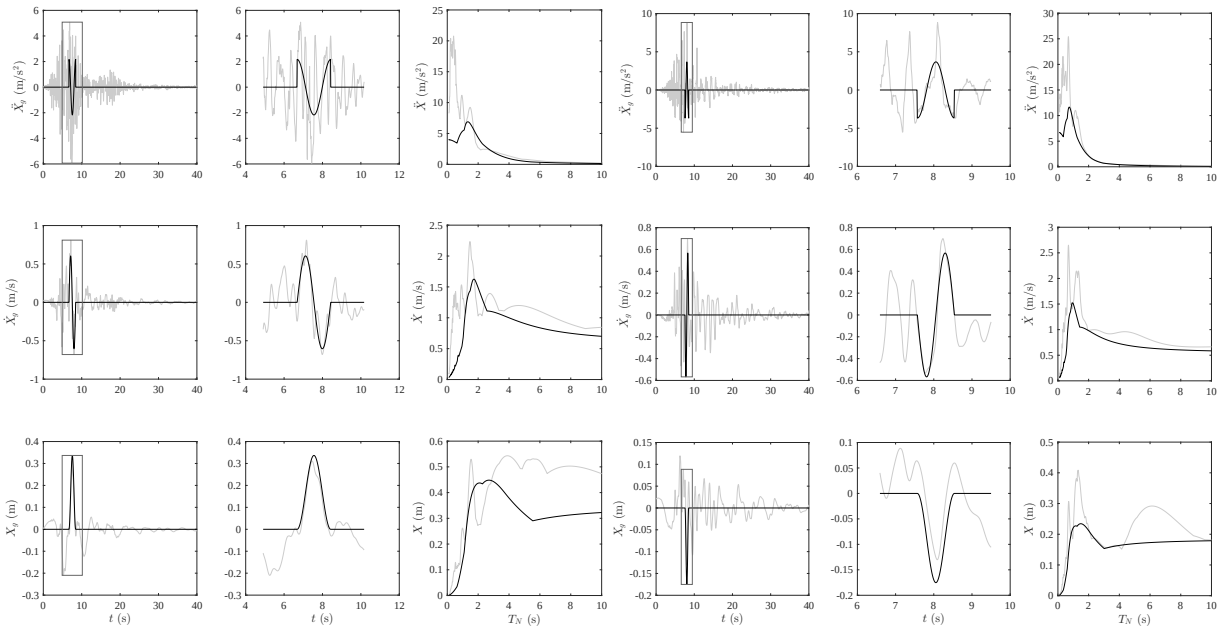

Figure 7: Identified pulse for the KMM006 record

Figure 8: Identified pulse for the KMM008 record

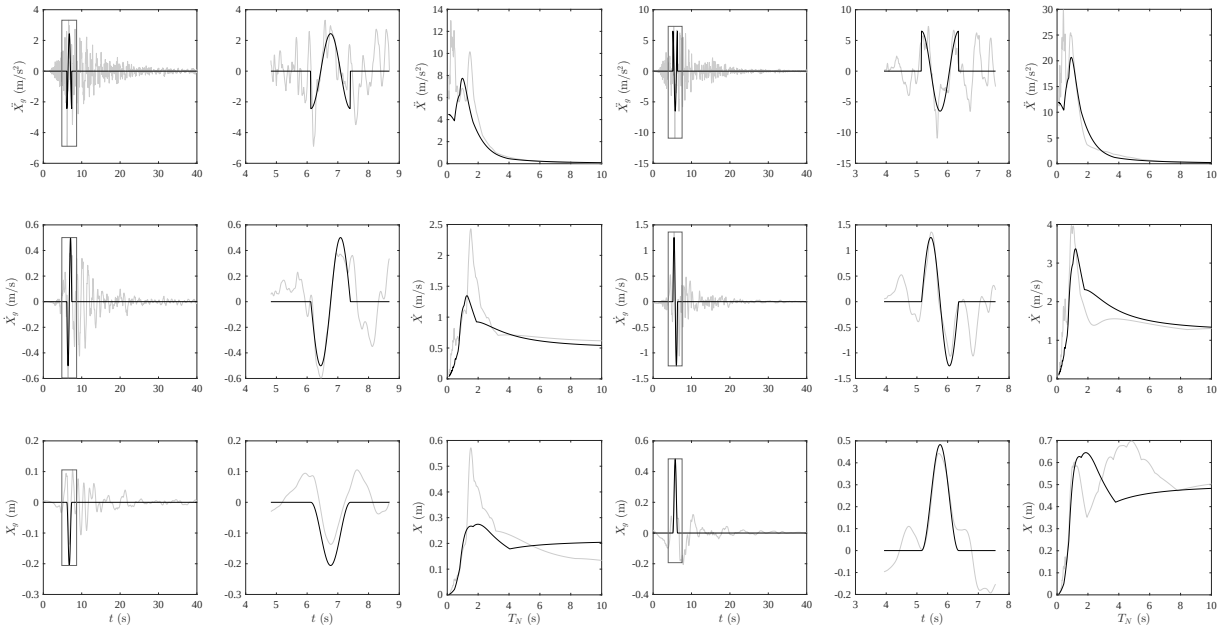

Figure 9: Identified pulse for the KMMH14 record

Figure 10: Identified pulse for the KMMH16 record

7) Jonathan D. Bray and Adrian Rodriguez-Marek. Characterization of forward-directivity ground motions in the near-fault region. *Soil Dynamics and Earthquake Engineering*, 24(11):815–828, December 2004. ISSN 02677261. doi: 10.1016/j.soildyn.2004.05.001. URL http://linkinghub.elsevier.com/retrieve/pii/S0267726104000703.

8) J. W. Baker. Quantitative Classification of Near-Fault Ground Motions Using Wavelet Analysis. *Bulletin of the Seismological Society of America*, 97(5):1486–1501, October 2007. ISSN 0037-1106. doi: 10.1785/0120060255. URL http://www.bssaonline.org/cgi/doi/10.1785/0120060255.